

# Journal of Vibration and Control

<http://jvc.sagepub.com>

---

## **Adaptive Running of a Quadruped Robot Using Forced Vibration and Synchronization**

Zu Guang Zhang, Hiroshi Kimura and Kunikatsu Takase

*Journal of Vibration and Control* 2006; 12; 1361

DOI: 10.1177/1077546306070596

The online version of this article can be found at:

<http://jvc.sagepub.com/cgi/content/abstract/12/12/1361>

---

Published by:

 SAGE Publications

<http://www.sagepublications.com>

**Additional services and information for *Journal of Vibration and Control* can be found at:**

**Email Alerts:** <http://jvc.sagepub.com/cgi/alerts>

**Subscriptions:** <http://jvc.sagepub.com/subscriptions>

**Reprints:** <http://www.sagepub.com/journalsReprints.nav>

**Permissions:** <http://www.sagepub.com/journalsPermissions.nav>

**Citations** (this article cites 12 articles hosted on the SAGE Journals Online and HighWire Press platforms):  
<http://jvc.sagepub.com/cgi/content/abstract/12/12/1361#BIBL>

# Adaptive Running of a Quadruped Robot Using Forced Vibration and Synchronization

ZU GUANG ZHANG

*Department of Precision Engineering, Graduate School of Engineering, The University of Tokyo, 7-3-1 Hongo, Bunkyo-ku, Tokyo 113-8656, Japan (hero@intellect.pe.u-tokyo.ac.jp)*

HIROSHI KIMURA

KUNIKATSU TAKASE

*Department of Information Management Science, Graduate School of Information Systems, The University of Electro-Communications, 1-5-1 Chofugaoka, Chofu City, Tokyo 182-8585, Japan*

(Received 7 December 2005; accepted 4 May 2006)

*Abstract:* In this paper we regard legged locomotion (e.g., running) as adaptive vibration, which is capable of adapting to changes in internal parameters and in the external environment. We propose control concepts for such adaptive running in general, and present a theoretical study of the bounding locomotion of a quadruped robot according to the proposed control concepts. In our control method, a forced vibratory system with a synchronization function is constructed by using a rhythm generator and a torque generator. The states of both generators are modified by delayed feedback control (DFC) using a stance phase period measured by contact sensors. Such sensory feedback to both generators makes the system adaptive to changes in the physical parameters and also adaptive to changes in terrain. The effectiveness of the proposed method was confirmed by simulations using a quadruped robot with an active hip joint and a passive knee joint in each leg. MPEG footage of these simulations can be seen at: <http://www.kimura.is.uec.ac.jp/running>.

*Keywords:* Quadruped robot running, forced vibration, synchronization, delayed feedback control

## 1. INTRODUCTION

Among researchers who have studied the running of legged robots, Raibert's monopod, biped and quadruped robots are well known (Raibert, 1985). Motivated by Raibert's success, many studies have been conducted on the running of legged robots. Since the 1990s, there has been progress in the stability analysis of one-legged hopping and in the development of hopping robots (Koditschek and Buehler, 1991; Vakakis et al., 1991; Ahmadi and Buehler, 1997; Hyon and Mita, 2002). By simulating the marvelous mobility of four legged mammals, various control strategies for quadruped running have been explored in simulation studies (Berkemeier, 1998; Krasny and Orin, 2004; Herr and McMahon, 2000; Palmer et al., 2003; Poulakakis et al., 2003) and experiments (Furusuo et al., 1995; Kimura et al., 1999; Poulakakis et al., 2005b; Zhang et al., 2003).

*Journal of Vibration and Control*, **12(12)**: 1361–1383, 2006

©2006 SAGE Publications

DOI: 10.1177/1077546306070596

However, studies of autonomous dynamic adaptation, allowing a robot to cope with infinite variation of terrain, have begun only recently, and are being performed by only a few research groups. One example is the recent achievement of high-speed mobility of a hexapod over irregular terrain with appropriate mechanical compliance of the legs (Saranli et al., 2001; Cham et al., 2004). The purpose of this study is to produce adaptive running for various states or terrains using a mammal-like quadruped robot.

For efficient running, a quadruped robot must have an energy-restoring system such as a spring mechanism. In such cases, running can be considered to be a vibration adapting to changes in internal parameters and the external environment. When running is considered as a vibration, the dynamic properties of the mechanism are important. We should consider that running motion and running control take advantage of such dynamic properties. In this paper, we first consider quasi-passive running in a bounding gait with no energy loss, and use a fixed point of a Poincaré map as the desired motion. Steady running at a fixed point has two advantages that utilize the dynamic properties of the mechanism. These are energy efficiency and self-stability (Blickhan, 1989; Serfarth et al., 2002). To cause the motion of a quadruped robot to converge to one fixed point in the presence of energy loss and disturbance, we next employ a rhythm generator and a torque generator combined with sensory feedback that we refer to as delayed feedback (Osuka et al., 2004). We use the stance phase period measured by contact sensors with practical levels of accuracy. This original method autonomously generates energy-efficient running with self-stabilizing ability against disturbances causing no energy loss, and generates adaptation ability against disturbances causing energy loss. As a result, the running motion considered in this paper is forced vibration with synchronization. The effectiveness of the proposed method is confirmed by simulations using a quadruped robot with an active hip joint and a passive knee joint in each leg.

In contrast with Raibert's (1985) control strategy, we do not directly utilize the forward speed, the jump height or the pitch angle of the body as measured by sensors. As a result, our proposed control method is simpler and more robust. In addition, it is important to mention here that the structure of the proposed controller is clearer and more practical for the generation of a bounding gait than that proposed by Poulakakis et al. (2005a) in two respects. First, the running converges to a definite fixed point. Second, mechanisms capable of stabilizing the gait and energy are explicitly integrated.

## 2. CONCEPTS FOR ADAPTIVE RUNNING

Legged locomotion can be considered to be vibration that adapts to changes in internal parameters and in the external environment. Ono and Okada (1994) indicated that such adaptive vibration can be generated by two types of systems; a self-excited vibratory system, or a combined system with forced vibration and synchronization. Self-excited vibration is good for adapting to changes in internal parameters (e.g., leg length, stiffness and viscosity), but it is inadequate for adjustments of stride and speed and for adaptation to the external environment. On the other hand, forced vibration itself has no adaptability. Thus, synchronization is necessary for the system to adapt to changes in internal parameters and in the external environment.

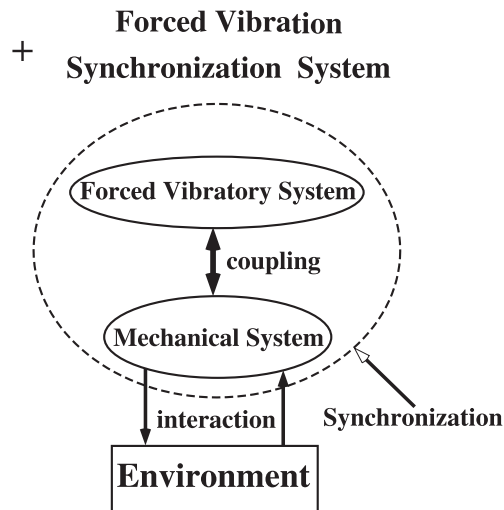


Figure 1. Legged locomotion generation and adaptation using a combined forced vibration and synchronization system.

Full and Koditschek (1999) pointed out that rhythmic motion is mainly generated by the spring-mass system in high-speed running, and that the self-stabilization property of a mechanism can cancel disturbances. In other words, self-excited or forced vibration without synchronization is sufficient for running in steady state. However, synchronization ability will play an important role in transient states such as the transition from standing to steady running, running up steps and so on.

Legged locomotion generated by forced vibration and synchronization is illustrated in Figure 1. The forced vibratory system and the mechanical system (i.e., a quadruped robot with compliant legs) have their own nonlinear dynamics. These two dynamic systems are coupled to each other, and can generate locomotion by interacting with the environment emergently and adaptively (Taga et al., 1991; Fukuoka et al., 2003). We called this method forced vibration and synchronization based locomotion. In this method, there is no difference between motion generation and adaptation. The forced vibration and synchronization system can induce autonomous adaptation according to its own dynamics in response to changes in the environment (e.g., adaptive running on irregular terrain).

In this paper, we propose a new legged locomotion generation and adaptation method, taking the following issues into account:

1. Whether we can construct a system in which the spring-mass system is dominant in a steady state and the forced vibration and synchronization system works in transient states;
2. Whether we can design a forced vibratory system which has no natural cyclic period and can be synchronized with the natural cyclic period of the spring-mass system;
3. What kind of sensory information is appropriate for adaptive running while considering some difficulties from an engineering point of view (e.g., noise and drift).

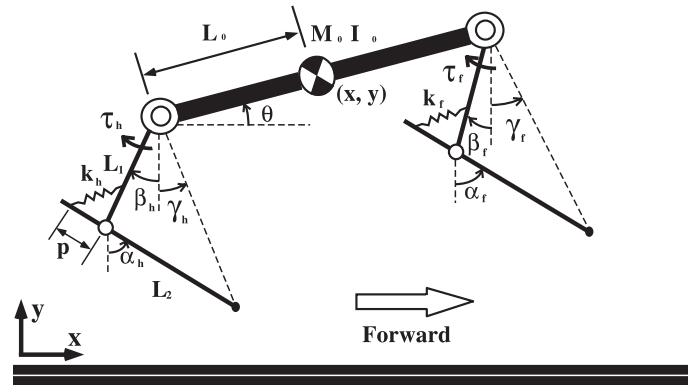


Figure 2. Sagittal plane model of a quadruped robot.

### 3. UTILIZING NATURAL DYNAMICS OF MECHANICAL SYSTEMS

In order to realize the forced vibration and synchronization based locomotion generation which works with the natural dynamics of a mechanism, we first numerically analyze the self-stability in quasi-passive running of a quadruped robot.

We present a number of sagittal plane models for construction of a hybrid quadruped bounding system in Section 3.1. In each case, the corresponding equations of motion are derived based on the Lagrangian method. Moreover, we introduce several self-stabilizing properties by seeking the fixed point of a Poincaré map modeling the bounding cycle, as described in Section 3.2 and Section 3.3. Although an identical analysis has been studied in a conservative model of Scout II (Poulakakis et al., 2003), we seek the fixed points and re-confirm the self-stabilizing property in our quadruped bounding system, which uses different mechanisms from Scout II.

#### 3.1. Definition of the Hybrid Quadruped Bounding System

A sagittal plane compliant model, as shown in Figure 2, is used to analyze running of the quadruped. The model is composed of a rigid body and a pair of spring-loaded two-segment legs. The center of gravity of the body is located at the center of the body link  $(x, y)$ . The mass, moment of inertia, length and pitch angle of the body are  $M_0$ ,  $I_0$ ,  $2L_0$  and  $\theta$ , respectively. The suffixes  $f$  and  $h$  represent the forelegs and hind legs, respectively. The angle of the hip joint with respect to the toe is  $\gamma_l$  ( $l = \{f, h\}$ ).  $k_l$  is the spring constant. The knee joints are always passive.

Several assumptions form the basis for the modeling and analysis of bounding locomotion:

1. The bounding locomotion is primarily planar. The velocity of a robot's components in directions perpendicular to the plane of progression are typically small for quadruped running gaits. Our models and analysis will therefore be constrained to the sagittal plane;

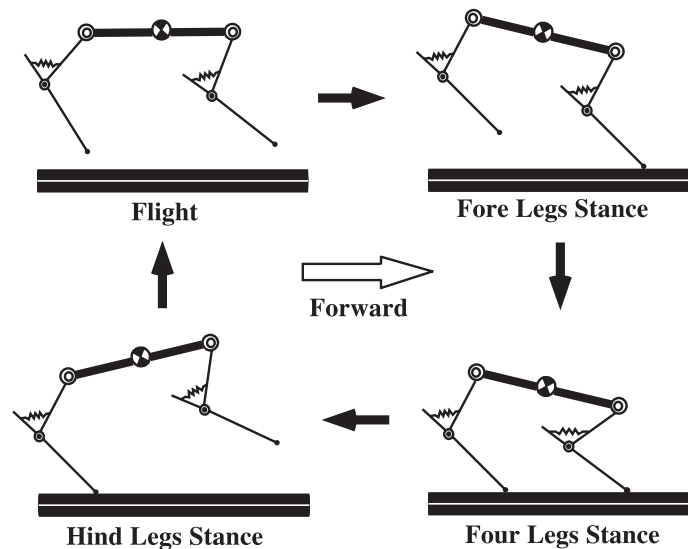


Figure 3. Phase transitions of the sagittal plane bounding gait. This bounding gait contains four phases (flight, forelegs stance, four legs stance and hind legs stance).

2. The leg mass is negligible relative to the body mass. It is assumed that the leg mass is sufficiently small for their effect on the body dynamics to be limited to the transmission of the ground reaction forces at the toes to the body when they are in contact with the ground. This assumption is a fairly accurate approximation as a result of the very light legs on our experimental platform;
3. The toe will be treated as a frictionless pin joint when it is in contact with the ground. This implies that no slipping between the toe and the ground occurs and that the toe makes point contact with the ground;
4. The friction in each joint and between the leg and ground is negligible. The energy loss can be avoided so that the whole system satisfies the energy conservation principle.

In light of these assumptions, the leg can be arbitrarily placed during the swing phase period at no energetic cost, and the collision equations of the legs with the ground can be omitted from the definition of the hybrid quadruped bounding system.

The quadruped bounding system consists of four phases (flight, forelegs stance, four legs stance and hind legs stance) in one cycle of running (see Figure 3), where only one flight phase, the “extended flight phase” (Krasny and Orin, 2004), appears after the hind legs stance phase. In all phases, we choose the same parameterization of the configuration space: By the Cartesian coordinates of the mass center of the body ( $x$ ,  $y$ ) and the orientation of the body in the inertial frame,  $\theta$ . In each phase, the equation of motion is

$$\mathbf{M}(\mathbf{x})\ddot{\mathbf{x}} = \mathbf{H}(\mathbf{x}, \dot{\mathbf{x}}) + \mathbf{F}_{el} + \mathbf{G}, \quad (1)$$

where  $\mathbf{x} = [x, y, \theta]^T$ ,  $\mathbf{M}$  is the inertia matrix and  $\mathbf{H}$ ,  $\mathbf{F}_{el}$  and  $\mathbf{G}$  are the vectors of the Coriolis, elastic and gravitational forces, respectively. The geometric constraints as transition conditions for touchdown and lift-off events are

$$\begin{aligned}
 &\text{swing} \implies \text{stance} \\
 &y^{td} \pm L_0 \sin \theta \leq L_1 \cos \beta_l^{td} + L_2 \cos \alpha_l^{td} \\
 &\text{stance} \implies \text{swing} \\
 &\delta_l = \delta_{l0}, \quad (\delta_l = \pi - \beta_l - \alpha_l)
 \end{aligned}
 \tag{2}$$

where  $l = \{f, h\}$  for the fore (+ in equation (2)) and hind (− in equation (2)) legs respectively.  $y^{td}$  is the height of the center of the body at the touchdown moment.  $\delta_{l0}$ , which is defined as 2.095 rad in this study, represents the initial posture of the two-link leg.

### 3.2. Searching for Fixed Points

Steady rhythmic locomotion can be formulated by defining a return map called a Poincaré map and achieved by stabilizing the discrete dynamical system expressed by the Poincaré map. Specifically, in our study, we first choose the state variables at the apex height in the flight phase  $\mathbf{p} = [y_p, \theta_p, \dot{x}_p, \dot{\theta}_p]^T$ , as a reference point of the Poincaré map and use the touchdown angles of the forelegs and hind legs  $\mathbf{q} = [\gamma_f^{td}, \gamma_h^{td}]^T$  as the control inputs of the system. Next, we integrate the equations of motion of all the phases in one bounding cycle from initial states at the  $n^{th}$  apex height by using an adaptive step 4<sup>th</sup> order Runge-Kutta routine in MATLAB. This process yields the state variables at the  $(n + 1)^{th}$  apex height, which is the value of the Poincaré map calculated at the  $n^{th}$  apex height. This relationship can be formulated as follows:

$$\mathbf{p}[n + 1] = \mathcal{P}(\mathbf{p}[n], \mathbf{q}[n]).
 \tag{3}$$

Finally, in order to obtain repetitive and cyclic bounding, we seek conditions for which the resulting state variables at the new apex height are identical with the initial state variables. In the field of nonlinear dynamics, the state variable that satisfies the equilibrium conditions is called a fixed point. To find a fixed point in equation (3) that maps on to itself, the following equation is solved

$$\mathbf{p} - \mathcal{P}(\mathbf{p}) = \mathbf{f}(\mathbf{p}) = 0,
 \tag{4}$$

for all reasonable values of touchdown angle. In our study, we utilize the simplest multidimensional root finding method, the Newton-Raphson method, to seek an approximation of the asymptote of equation (4). Here,  $\mathbf{f}(\mathbf{p})$  can be expanded in a Taylor series

$$\mathbf{f}(\mathbf{p} + \delta\mathbf{p}) = \mathbf{f}(\mathbf{p}) + \mathbf{J} \cdot \delta\mathbf{p} + \mathcal{O}(\delta\mathbf{p}^2).
 \tag{5}$$

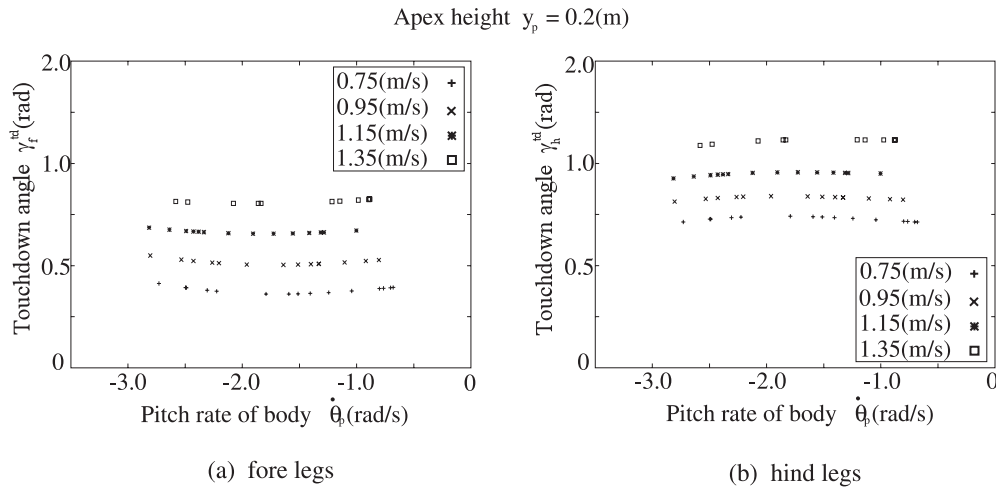


Figure 4. Fixed points for various forward speeds (between 0.75 m/s and 1.35 m/s) and constant apex height (0.2 m).

By neglecting terms of order  $\delta\mathbf{p}^2$  and higher, and by assuming that  $\mathbf{f}(\mathbf{p} + \delta\mathbf{p})$  is nearing 0, we obtain a linear equation (equation (6)) for the corrections  $\delta\mathbf{p}$  that moves each function closer to zero simultaneously.

$$\mathbf{J} \cdot \delta\mathbf{p} = -\mathbf{f}(\mathbf{p}). \tag{6}$$

Matrix equation (6) can be solved by LU decomposition. The corrections are then added to the solution vector

$$\mathbf{p}_{new} = \mathbf{p}_{old} + \delta\mathbf{p}, \tag{7}$$

and the process is iterated until convergence. In general, it is a good idea to check the degree at which all variables have converged. Once either variable reaches machine accuracy, the other will cease to change. We set the machine accuracy to  $1e-6$  during a complete bounding cycle.

A large number of fixed points of the Poincaré map for different initial conditions and different touchdown angles have been searched. Figure 4 shows the fixed points as the forward speed varies between 0.75 m/s and 1.35 m/s while the apex height is kept constant (at 0.2 m). In addition, the stabilities of these fixed points have been studied by seeing whether all the eigenvalues of the Jacobian matrix (equation (8)) relating to the equilibrium status  $(\mathbf{p}^*, \mathbf{q}^*)$  have magnitude less than one.

$$\mathbf{J} = \frac{\partial \mathcal{P}(\mathbf{p}^*, \mathbf{q}^*)}{\partial \mathbf{p}}. \tag{8}$$

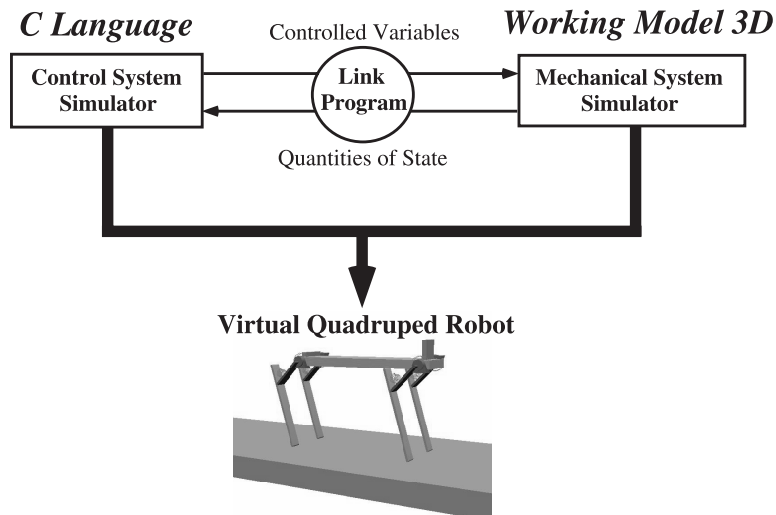


Figure 5. The composition of the hybrid simulator. The mechanical system simulator is constructed in *Working Model 3D*, and the control system simulator is described in the C language.

Table 1. The characteristics of the fixed point  $\mathbf{p}^*$  used in the simulations.  $y_p$ ,  $\theta_p$ ,  $\dot{x}_p$  and  $\dot{\theta}_p$  are the height, pitch inclination, forward speed and pitch rate of the body at the apex, respectively.

|                       |                                |                          |       |
|-----------------------|--------------------------------|--------------------------|-------|
| $y_p$ (m)             | 0.2                            | $\theta_p$ (rad)         | 0     |
| $\dot{x}_p$ (m/s)     | 0.95                           | $\dot{\theta}_p$ (rad/s) | -1.52 |
| $\gamma_f^{td}$ (rad) | 0.524                          | $\gamma_h^{td}$ (rad)    | 0.838 |
| energy (J)            | 1.36                           | cyclic period (s)        | 0.292 |
| eigenvalues of $J$    | 0.0003, 0.0005, -0.032, 0.0213 |                          |       |

### 3.3. Self-Stability of Quadruped Bounding System

In this paper, we adopt  $\mathbf{p}^* = [0.2, 0, 0.95, -1.52]^T$  as a typical fixed point and use the touchdown angles  $\mathbf{q}^* = [0.524, 0.838]^T$  corresponding with this fixed point. Since all the eigenvalues of its Jacobian matrix have magnitude less than one as shown in Table 1, the typical fixed point can be regarded as an asymptotically stable fixed point. Other quantities related to this fixed point are also shown in Table 1.

In order to demonstrate that the self-stabilizing property can still work effectively even when friction and collision cause energy loss, we have chosen to study the more practical bounding, approximating an actual robot where, unlike the quasi-passive running model, the leg mass, moment of inertia, viscous friction in each joint, and collision between legs and the ground are considered. Thus, we build a more accurate simulator by using a combination of *Working Model 3D* and the C programming language (see Figure 5). For one thing, we

Table 2. The parameter values used for the quadruped physical model.  $c_{hip}$  and  $c_{knee}$  indicate the viscous friction coefficients at the joints.  $\alpha_0$  and  $\beta_0$  represent the joint angles of the knee and hip joints in the initial standing posture.

| parameters          | value | parameters               | value       |
|---------------------|-------|--------------------------|-------------|
| $M_0$ (kg)          | 1.12  | $I_0$ ( $\text{kgm}^2$ ) | $5.5E - 2$  |
| $M_1$ (kg)          | 0.35  | $I_1$ (kg)               | $2.05E - 4$ |
| $M_2$ (kg)          | 0.12  | $I_2$ ( $\text{kgm}^2$ ) | $2.31E - 4$ |
| $L_0$ (m)           | 0.15  | $L_1$ (m)                | 0.08        |
| $L_2$ (m)           | 0.15  | $p$ (m)                  | 0.03        |
| $k_f$ (kN/m)        | 20    | $k_h$ (kN/m)             | 20          |
| $c_{hip}$ (Nms/rad) | 0.017 | $c_{knee}$ (Nms/rad)     | 0           |
| $\alpha_0$ (rad)    | 0.685 | $\beta_0$                | 0.812       |

construct the mechanical system of the model in *Working Model 3D* and describe the control system in the C language. The simulator was built by combining the mechanical and control systems using a special linking program. Note that the inelastic collision model implemented in *Working Model 3D* is used in the following simulations. The parameters of the quadruped model are shown in Table 2.

In this simulation, the quadruped robot first begins to run from an initial condition that satisfies the state variables of the asymptotically stable fixed point as given in Table 1. Second, a small and temporary disturbance (0.034 rad) of the touchdown angle in the hind leg during the swing phase period appears after 2 s. Here, the control system decides the phase (i.e., stance or swing) of each leg based on measurements from contact sensors located in the robot's feet. During the stance phase period, appropriate constant torque capable of sustaining stable bounding (Zhang et al., 2005) is output by actuators in the hip joints. A PD controller driving the touchdown angle to a desired value is engaged during the swing phase period. As shown in Figure 6, the forward speed increases (A) and the apex height decreases (B) when the disturbance of the touchdown angle occurs. Because of the self-stabilizing property, the bounding finally converges upon a fixed point similar to the initial condition. Even though friction and collision cause energy loss from the system in this simulation, the self-stability of the quadruped bounding system is capable of suppressing the disturbance where there is no potential energy change relative to the touchdown plane. Indeed, there exists a regime where the quadruped bounding system can stabilize the forward speed and jump height itself without directly measuring these state variables simply by driving the touchdown angles of the legs to the desired values. This fact could provide a significant hint as to how to simplify control.

In the light of the above consideration, we conclude that a fixed point with the self-stabilizing property is very appropriate as the desired steady state. The fixed point described in Table 1 will therefore also be used as the desired steady state when the sensory feedback is introduced in following sections.

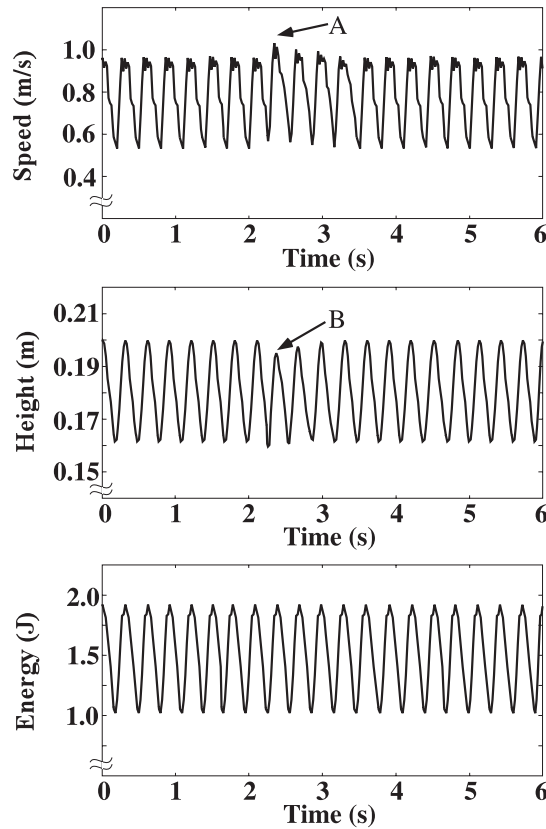


Figure 6. The simulation results for running with friction and collision on a flat floor with disturbance to the touchdown angle of the hind leg. In the stance phase, the actuators' output torque is calculated by energy reference control (Zhang et al., 2005). Depending on the self-stability, the robot stabilizes bounding locomotion.

#### 4. IMPLEMENTATION OF A FORCED VIBRATION AND SYNCHRONIZATION SYSTEM

The above-mentioned facts concerning self-stabilizing properties provide insight into the basic stabilization regime of a quadruped running system in terms of forward speed, jump height and touchdown angle. Even though the stabilization regime arises from an analysis relating to unactuated and conservative dynamics, it provides a significant guideline for the design of a control method. In an actual robot, if we can reasonably compensate for the energy loss caused by friction and collision, the robot may depend on the basic stabilization regime to realize stable bounding as it would in a conservative system.

#### 4.1. Engineering Limitations on Sensory Feedback

In general, in order to realize the above-mentioned compensation for lost energy, use of an energy-based control method would be considered. For an energy-based control method, reliable knowledge of the system energy is vitally important. However, when measuring the forward speed or jump height, which are essential parameters for the calculation of the system energy, through a combination of several sensors, we have to confront such difficulties as integration error, noise and drift. Since it is difficult to accurately calculate and measure the system energy in an actual robot, the energy-based control method appears unsuitable for practical application. Thus, to use our control method for quadruped bounding, we need to use a practical sensory feedback system that can overcome sensory measurement limitations.

As outlined in the work of Cham et al. (2004), it is much easier to measure the stride period through a binary switch attached to the feet of a robot than to measure the inclination of the body using an angular velocity sensor or the forward speed with an acceleration sensor. Cham et al. achieved high-speed running of a hexapod robot over various types of terrain by adjusting the stride period as measured by a binary switch. Motivated by this idea, we also selected the stance phase period, measured using a contact sensor, as sensory feedback in our study.

#### 4.2. Motion Generation and Adaptation

From our current knowledge, it seems reasonable to hypothesise that the rhythm and gait of running locomotion will be governed by the spring-mass system in the steady state (e.g., stable running), and generated and adjusted by the rhythm generator in the transient state (e.g., shifting from the standing state to the stable bounding state or running up a small step). Thus, we design a rhythm generator capable of adjusting the period and phases of running locomotion so as to easily generate a stable running rhythm with the required gait (e.g., stable bounding) via the proposed control method.

On the other hand, the stabilization of rhythmic locomotion (e.g., walking and running) can be considered to be a control issue concerning convergence upon a fixed point. It is similar to the concept of delayed feedback control (DFC) in the field of chaotic control. Following up on this research, Osuka et al. (2004) selected the kinetic energy on the impact point as the controlled variable used by the DFC method to stabilize bipedal quasi-passive-dynamic-walking in simulations. However, since an energy-based controller is inadequate when it comes to practical application, as described in Section 4.1, we modified Osuka's DFC method and propose our original control method of quadruped bounding for an actual robot.

##### 4.2.1. Rhythm Generator

We define the phase  $\phi_l$  of each leg in the  $n^{\text{th}}$  step as given by equation (9). Here, the robot uses the leg phase to switch the torque generator:

$$\phi_l = \sin(\omega_l[n]t + \psi_l) + \phi_{0l}, \quad \omega_l[n] = \frac{2\pi}{T_l[n]}. \quad (9)$$

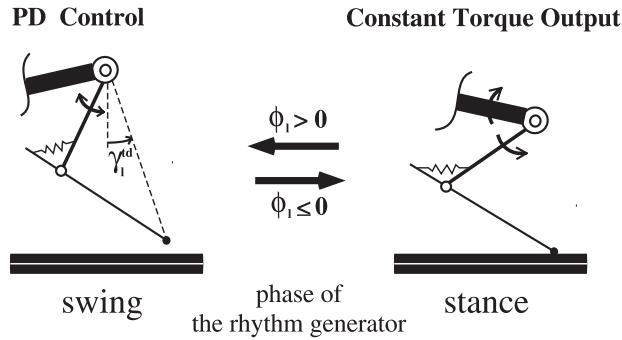


Figure 7. Switching of the hip joint controller according to the output phase  $\phi_l$  of the rhythm generator.

Where  $T_l[n]$  and  $\omega_l[n]$  are the cyclic period and the angular frequency of the leg  $l$  in the  $n^{\text{th}}$  step, respectively. The initial phase  $\psi_l$  is defined for the generation of the gait. (Where  $\psi_f = 0$ ,  $\psi_h = \pi$  for the bounding gait and  $\psi_f = \pi$ ,  $\psi_h = \pi$  for the prancing gait, where 0 and  $\pi$  mean that the leg begins to move from the swing phase and stance phase, respectively.) The offset  $\phi_{0l}$  determines the duty factor.  $T_l[n]$  is calculated by using the DFC method described in Section 4.2.3. The timing for each leg to switch between the stance and swing phase is:  $\phi_l > 0$ : swing phase,  $\phi_l \leq 0$ : stance phase (Figure 7).

#### 4.2.2. Torque Generator

Depending on the leg phase  $\phi_l$  generated by the rhythm generator, the following different control actions are assigned as shown in Figure 7: In the swing phase ( $\phi_l > 0$ ), the PD control expressed by equation (10) is performed;

$$\tau_l(t) = -K_p(\gamma_l - \gamma_l^{td}) - K_d\dot{\gamma}_l \quad (10)$$

in the stance phase ( $\phi_l \leq 0$ ), constant torque  $\tau_l^{st}[n]$  of the hip joint in each leg is output, as expressed by equation (11).

$$\tau_l(t) = \tau_l^{st}[n]. \quad (11)$$

In the control action of the swing phase,  $\gamma_l^{td}$  is the touchdown angle corresponding with the fixed point (Table 1).  $K_p$  and  $K_d$  are the gains of the PD control. In the control action of the stance phase, the DFC method described in Section 4.2.3 determines  $\tau_l^{st}[n]$ .

#### 4.2.3. Convergence upon a Fixed Point based on DFC

The properties of delayed feedback control motivate the control method of quadruped bounding described here. It is advantageous to use a DFC method that results in a steady-state cycle. As outlined in the previous section, we use the stance phase period to provide the sensory

Table 3. The parameter values of the controller used in simulations.

| parameters            | value | parameters            | value |
|-----------------------|-------|-----------------------|-------|
| $\psi_f$              | 0     | $\psi_h$              | $\pi$ |
| $\phi_{0f}$           | 0.16  | $\phi_{0h}$           | 0.09  |
| $\gamma_f^{td}$ (rad) | 0.524 | $\gamma_h^{td}$ (rad) | 0.838 |
| $K_{DF.T}$            | 0.12  | $K_{DF.\tau}$         | 6.8   |
| $K_p$ (N·m/rad)       | 1.2   | $K_d$ (N·ms/rad)      | 0.02  |

feedback for the DFC method since the stance phase period is easy to measure accurately. Hence, the proposed DFC methods are:

$$T_l[n+1] = T_l[n] - K_{DF.T}(t_l^{st}[n] - t_l^{st}[n-1]) \quad (12)$$

$$\tau_l^{st}[n+1] = \tau_l^{st}[n] - \delta(l)K_{DF.\tau}(t_l^{st}[n] - t_l^{st}[n-1]) \quad (13)$$

$$\delta(l) = \begin{cases} -1, & l = f : \text{foreleg} \\ 1, & l = h : \text{hindleg} \end{cases}$$

where  $K_{DF.T}$  and  $K_{DF.\tau}$  are the DFC gains, which are decided by trial and error in simulations. Equations (12) and (13) are used to calculate the cyclic period of the leg phase and the torque of the hip joint for the next stance phase, respectively. The parameters used by the control system in the following simulations are listed in Table 3.

## 5. SIMULATION RESULTS

### 5.1. Transition from Standing to Steady Bounding

We present here some simulation results for bounding running on flat terrain where the running locomotion shifts from the standing state to the steady bounding state. For these simulations, we use the touchdown angles corresponding with a fixed point of quasi-passive running, as listed in Table 1, and the associated parameters shown in Table 3 for the control system. In order to generate the bounding gait, we must decide the initial values of the DFC approach. Here, we adopt  $\{T_f[0], T_h[0], \tau_f[0], \tau_h[0]\} = \{0.20, 0.69, -1.0, 1.3\}$  as the initial condition of the DFC approach expressed by equation (12) and equation (13). As described in Section 4, the quadruped robot, according to  $\psi_l$ , begins to run with the initial condition in which forelegs are in the swing phase and hind legs are in the stance phase. In this case, the initial values of  $T_h[0]$  and  $\tau_h[0]$  are much larger than those in the steady state in order to provide sufficient kinetic energy during the first stance phase period of the hind legs. Figure 8 shows the forward speed, jump height and energy of the system as function of time. As shown in this figure, the apex height and forward speed in the steady state are similar to the state at the fixed point of quasi-passive running, as given in Table 1. In addition, the maximum heights of the toes (i.e., clearances) for the forelegs and hind legs are 3 cm and 2 cm, respectively. Figure 9 illustrates  $t_l^{st}[n]$ ,  $T_l[n]$ ,  $\tau_l^{st}[n]$  relating to the DFC approaches expressed by equation (12) and equation (13). As shown in this figure, the DFC approach

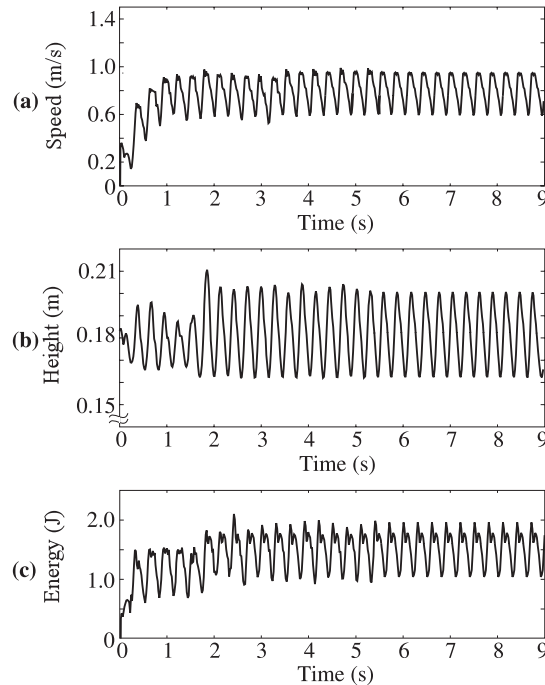


Figure 8. The simulation results of DFC in the transition from standing to steady running. (a) Forward speed  $\dot{x}$ , (b) height  $y$  and (c) total energy are shown.

based on the stance phase period change is capable of stabilizing the period of the rhythm generator and the torque of the hip joint during the stance phase period.

As shown in Figure 10, the running period  $T_l[n]$  generated by the rhythm generator accords with that measured by a contact sensor after the 20<sup>th</sup> step. At this point, the leg phases of the rhythm generator and motion are synchronized and converged on the bounding gait. Furthermore, the period and the leg phase difference in the steady state are the same as those of the fixed point. Consequently, it means that the rhythm generator and the practical motion are mutually synchronized by using the DFC approach expressed by equation (12), and the motion can be converged to a fixed point.

In this simulation, we treated the touchdown angle of each leg as the only feedback about the fixed point. We took advantage of the original DFC method by changing the stance phase period measured by contact sensors. Based on coupling between the forced vibration system and mechanical system, we achieved an autonomous transition from standing to steady bounding through the interaction between the robot's mechanism and the ground (see Figure 1). The steady state of bounding accorded with an asymptotically stable fixed point of quasi-passive running. In addition, torque was required in the steady state only to compensate for the energy loss caused by friction and collision. Consequently, the stable bounding generated can be considered to be efficient locomotion because it requires only a small amount of power and is less reliant on sophisticated real-time calculations or on substantial sensory feedback.

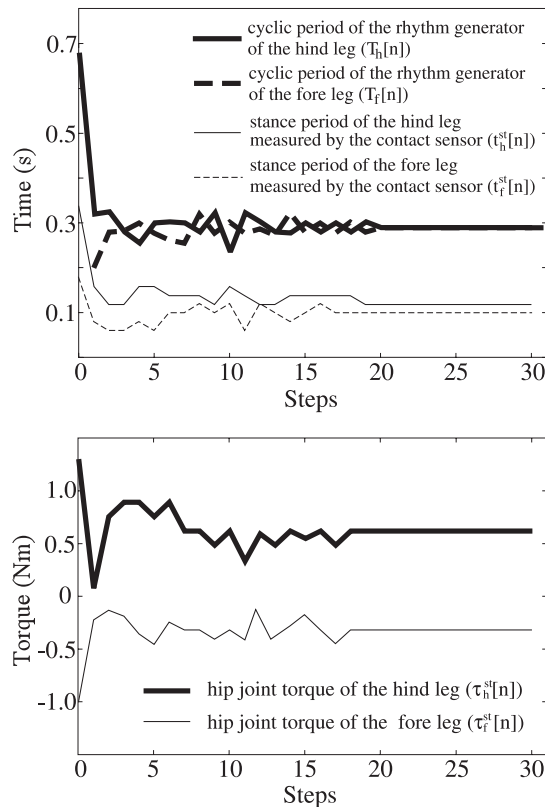


Figure 9. The simulation results of the DFC in the transition from standing to steady running. The parameter  $t_i^{st}[n]$  is measured using the contact sensor.  $T_i[n]$  and  $\tau_i^{st}[n]$  are calculated using equation (12) and equation (13), respectively. The period of a single step is approx. 0.29 s.

### 5.2. Convergence to a Fixed Point in the Presence of Errors

For practical applications, the robustness of the proposed control method to errors in the model is important. Figures 11 and 12 show the performance of three different quadruped robots going from standing to stable bounding. The physical parameters of robot1 have the values listed in Table 2. Robot2 and robot3 are similar to robot1 but with differences in the robot's mass, the spring constant, and the coefficient of viscosity in the hip joint. The mass, spring constant of the leg and coefficient of viscosity in the hip joint of robot1, robot2 and robot3 are 3 kg, 20 kN/m, 0.017 Nms/rad; 3.15 kg, 20.1 kN/m, 0.01785 Nms/rad; and 3.3 kg, 20.2 kN/m, 0.0187 Nms/rad, respectively, and robot2 and robot3 can be regarded as robot1 with model errors. As shown in Figure 11, with the initial conditions  $\{T_f[0], T_h[0], \tau_f[0], \tau_h[0]\} = \{0.20, 0.69, -1.0, 1.3\}$ , the forward speed and jump height of each robot converge upon a steady state under the proposed control method.  $T_i[n]$  and  $\tau_i^{st}[n]$  relating to the DFC method expressed in equation (12) and equation (13) are plotted in Figures 12 for the three robots examined. Since the rhythm generator and bounding motion

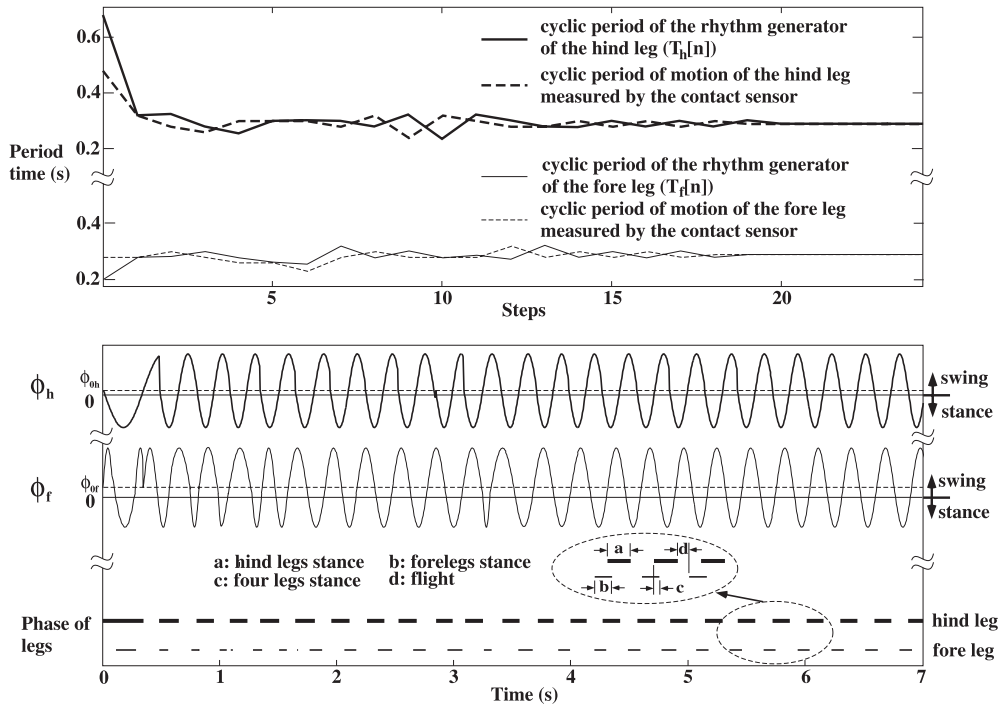


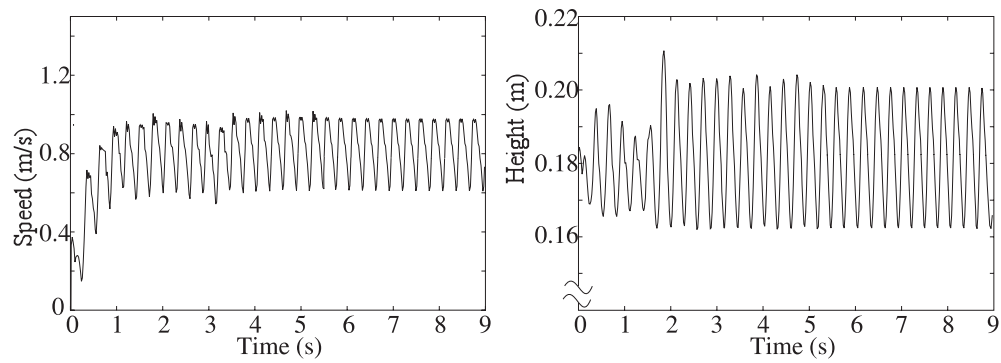
Figure 10. The simulation results of the DFC in the transition from standing to steady running. The cyclic period of the rhythm generator and the cyclic period of leg motion measured by the contact sensor are shown in the upper graph. The output phase of the rhythm generator and the phase of the leg measured by the contact sensor are shown in the lower graph. The period of a single step is approximately 0.29 s.

are mutually synchronized through DFC, the cyclic period of the rhythm generator and the torque of the hip joint in a stance phase can be stabilized. Examining Figures 11 and 12, we can see that the bounding of each of the three robots converges to a different fixed point, although the difference is very small. This indicates that the proposed control method enables the bounding motion of each quadruped robot to converge to another fixed point based on its own dynamics, in spite of using the pair of touchdown angles corresponding to the fixed point obtained using the model of the robot1.

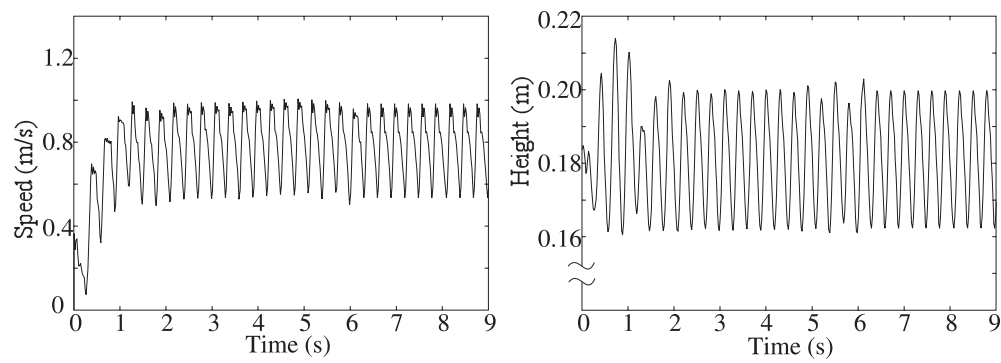
In addition, we have completed a number of such simulations where the robot’s physical parameters (e.g., mass, spring constant of the leg, length of the leg, length of the body, etc.) are changed to various values. The difference among the resulting fixed points is very small in the case the model errors of less than 5%, but the difference is very apparent with an error of 10% or more.

### 5.3. Role of Synchronization in the Proposed Method

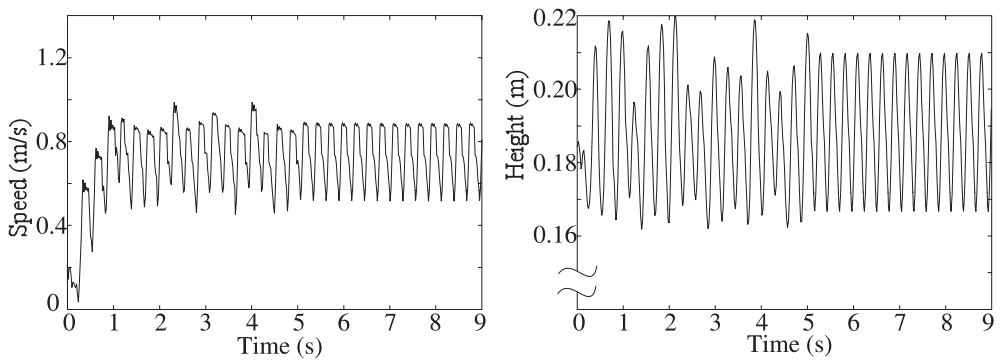
As described in Section 2, the synchronization ability should play an important role in transient states. In order to confirm the effectiveness of the synchronization function in the



(a) Robot 1



(b) Robot 2



(c) Robot 3

Figure 11. Performance tests relating to convergence on fixed points for quadruped robots with different physical parameters in the transition from standing to steady bounding. The period of a single step is approx. 0.29 s.

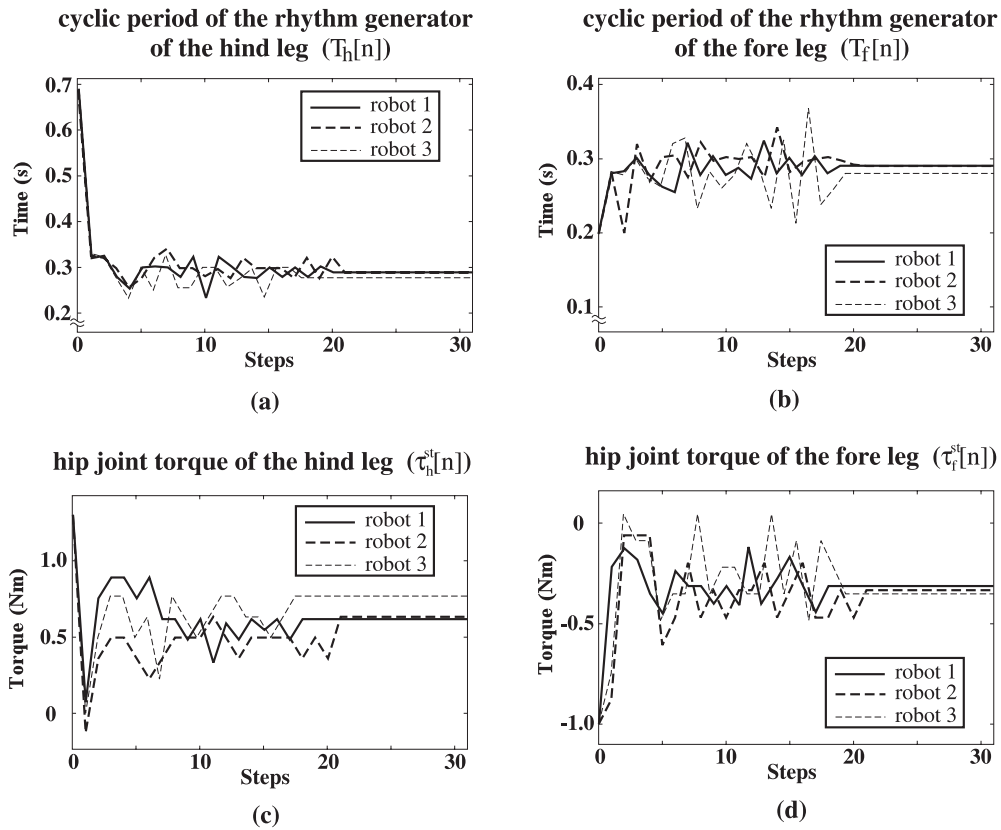


Figure 12. Performance tests relating to convergence on fixed points for quadruped robots with different physical parameters in the transition from standing to steady bounding.

rhythm generator, we attempted to generate a constant bounding pattern without DFC relating to the cyclic period of the rhythm generator outputting the leg phase (i.e., equation (12)). As a result of this, the cyclic periods of motion of the forelegs and hind legs cannot synchronize, and the running locomotion cannot converge to a stable bounding gait (see Figure 13).

#### 5.4. Running Up a Small Step

We will now use the proposed DFC approach described in Section 4.2 to conduct a simulation where the robot begins in the steady state and reaches a 2cm-height step after 2 s. As shown in Figure 15, since  $t_i^{st}[n]$  changes when the robot runs over the step in the 7<sup>th</sup> step, the DFC begins to work. More specifically, the DFC outputs larger torques for the hip joints in the hind legs (B) because of the longer stance phase period of the hind legs (A) in the 8<sup>th</sup> step, providing the necessary energy input (the energy change at about 2.3 s in Figure 14). After the transition states, the gait, torque and so on converge at the initial condition in the 17<sup>th</sup>

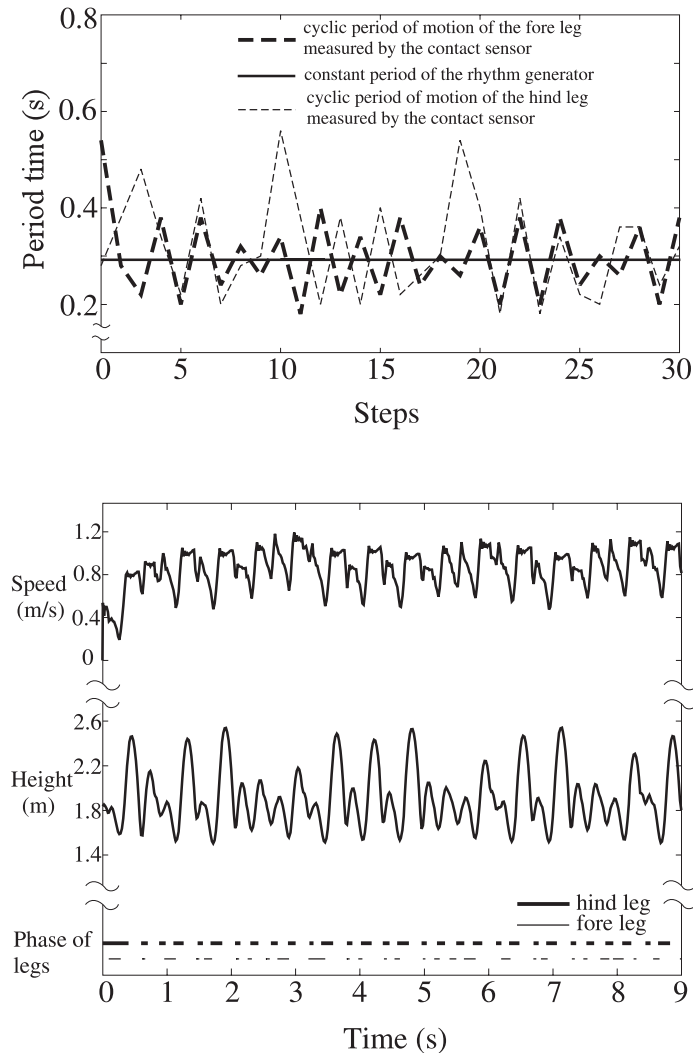


Figure 13. The simulation results in the transition from standing to steady bounding without DFC relating to the cyclic period of the rhythm generator. The cyclic periods of the rhythm generators of the four legs are held at 0.29s.

step. Figure 14 shows that the forward speed, jump-height and energy then re-converge at the initial condition after adjustments based on the DFC.

These results show that the proposed approach is capable of autonomously adapting to irregular terrain by treating the irregularity of the terrain as a temporary disturbance. However, when the energy relative to the touchdown plane regularly increases and decreases (e.g., the robot runs uphill and downhill), or when the robot runs over a big obstacle, additional control enabling state variables to transfer to other fixed points by adjusting the touchdown angle is necessary (Hyon and Emura, 2004).

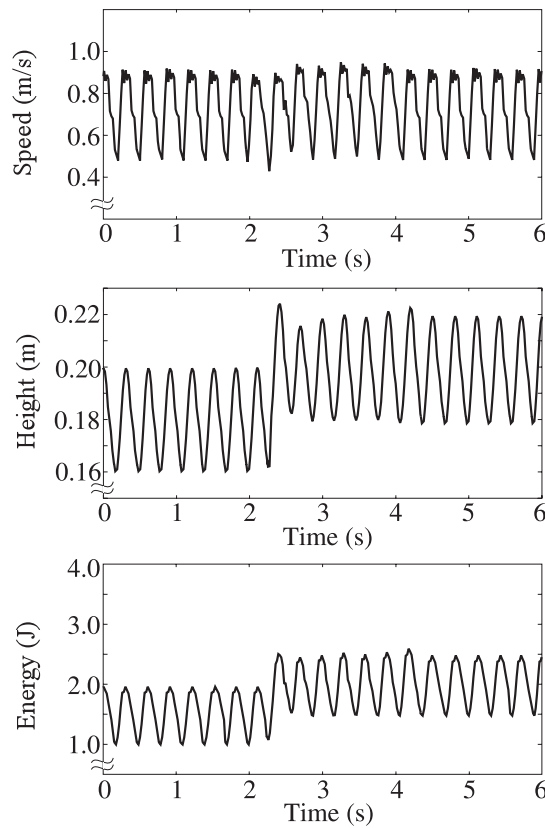


Figure 14. The simulation results of running over a 2cm-height step with DFC.

## 6. DISCUSSION

Poulakakis et al. (2005a) achieved transitions from standing to steady running in several running gaits with their quadruped robot without utilizing a rhythm generator by determining the constant torque needed to drive a leg to a sweep limit angle during the stance phase period and adopting a PD controller to drive a leg to a touchdown angle during the swing phase period. However, we indicate in Section 5 that the use of a rhythm generator in the control system of a quadruped robot brings several advantages to our study. First, our energy efficient stabilization method explicitly enables state variables to converge at the known asymptotically stable fixed point of quasi-passive running, while Poulakakis et al.'s method used a sweep limit angle and constant torque. Also, this rhythm generator, combined with our method for adjusting the torque of the hip joints in the stance phase, improves the robot's anti-disturbance capability. Of course, since the rhythm of motion is mostly generated by spring mechanisms during steady running, the role of the rhythm generator gradually becomes smaller as the motion approaches steady running. Consequently, the concept of forced vibration and synchronization described in Section 2 is valuable in the generation of adaptive running.

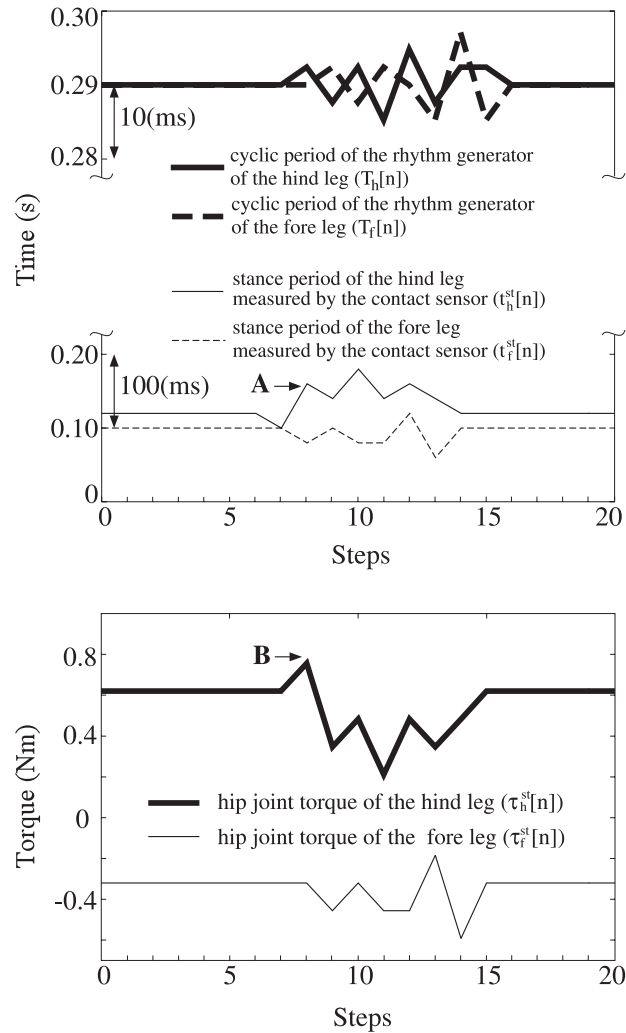


Figure 15. The simulation results for running up a 2cm-height step with DFC. The period of a single step is approx. 0.29 s. Note that the time scale is different between  $t_i^{st}[n]$  and  $T_i[n]$ .

## 7. CONCLUSION

In the forced vibration and synchronization system proposed in this study, the relationships between the components (rhythm generator, torque generator, sensory feedback and mechanism) were defined simply, and locomotion generation and adaptation were emergently produced by the coupled dynamics of a forced vibratory system (i.e., the rhythm generator and torque generator) and a mechanical system interacting with the environment. For synchronization, we applied a delayed feedback control to the rhythm and torque generators based on the stance phase period measured by contact sensors with practical levels of accuracy. Our simulations produced the following results:

1. The proposed original method generates stable running in a bounding gait with good energy efficiency utilizing natural dynamics.
2. Running motion as physical vibration is mutually synchronized with a rhythm generator as a forced vibration.
3. When a robot runs on flat terrain without any disturbance causing an energy loss, the self-stabilization property is sufficient.
4. When a robot runs up a small step, the energy relative to the touchdown ground is temporally changed. In such a case, the self-stabilization property is not sufficient, but the proposed DFC method is effective.
5. The spring-mass system is dominant in steady state, and the forced vibration and synchronization system plays an important role in transient states.

## REFERENCES

- Ahmadi, M. and Buehler, M., 1991, "Stable control of a simulated one-legged running robot with hip and leg compliance," *IEEE Transaction on Robotics and Automation* **13**(1), 96–104.
- Berkemeier, M.D., 1998, "Modeling the dynamics of quadruped running," *International Journal of Robotics Research* **17**(9), 971–985.
- Blickhan, R., 1989, "The spring-mass model for running and hopping," *Journal of Biomechanics* **22**, 1217–1227.
- Cham, J.G., Karpick, J.K., and Cutkosky, M.R., 2004, "Stride period adaptation of a biomimetic running hexapod," *International Journal of Robotics Research* **23**(2), 141–153.
- Fukuoka, Y., Kimura, H., and Cohen, A.H., 2003, "Adaptive dynamic walking of a quadruped robot on irregular terrain based on biological concepts," *International Journal of Robotics Research* **22**(3-4), 187–202.
- Full, R.J. and Koditschek, D.E., 1999, "Templates and anchors: Neuromechanical hypotheses of legged locomotion on land," *Journal of Experimental Biology* **202**, 3325–3332.
- Furusho, J., Sano, A., Sakaguchi, M., and Koizumi, E., 1995, "Realization of bounce gait in a quadruped robot with articular-joint-type legs," in *Proceedings of the 1995 IEEE International Conference on Robotics and Automation*, pp. 697–702.
- Herr, H.M. and McMahon, T.A., 2000, "A trotting horse model," *International Journal of Robotics Research* **19**(6), 566–581.
- Hyon, S.H. and Emura, T., 2004, "Energy-preserving control of a passive one-legged running robot," *Advanced Robotics* **18**(4), 357–381.
- Hyon, S.H. and Mita, T., 2002, "Development of a biologically inspired hopping robot 'Kenken'," in *Proceedings of the 2002 IEEE International Conference on Robotics and Automation*, pp. 3984–3991.
- Kimura, H., Akiyama, S., and Sakurama, K., 1999, "Realization of dynamic walking and running of the quadruped using neural oscillator," *Autonomous Robots* **7**(3), 247–258.
- Koditschek, D.E. and Buehler, M., 1991, "Analysis of a simplified hopping robot," *International Journal of Robotics Research* **10**(6), 587–605.
- Krasny, D.P. and Orin, D.E., 2004, "Generating high-speed dynamic running gaits in a quadruped robot using an evolutionary search," *IEEE Transactions on Systems, Man, and Cybernetics* **B34**(4), 1685–1696.
- Ono, K. and Okada, T., 1994, "Self-excited vibratory actuator (1<sup>st</sup> report: Analysis of two-degree-of-freedom self-excited systems)," *Transactions of the JSME(C)* **60**(577), 2984–2991.
- Osuka, K., Sugimoto, Y., and Sugie, T., 2004, "Stabilization of semi-passive dynamic walking based on delayed feedback control," (in Japanese) *Journal of the Robotics Society of Japan* **22**(2), 193–199.
- Palmer, L.R., Orin, D.E., Marhefka, D.W., Schmiechler, J.P., and Waldron, K.J., 2003, "Intelligent control of an experimental articulated leg for a galloping machine," in *Proceedings of the 2003 IEEE International Conference on Robotics and Automation*, pp. 3821–3827.
- Poulakakis, I., Papakopoulos, E., and Buehler, M., 2003, "On the stable passive dynamics of quadrupedal running," in *Proceedings of the 2003 IEEE International Conference on Robotics and Automation*, pp. 1368–1373.

- Poulakakis, I., Smith, J.A., and Buehler, M., 2005a, "Modeling and experiments of untethered quadrupedal running with a bounding gait: The Scout II robot," *International Journal of Robotics Research* **24**(4), 239–256.
- Poulakakis, I., Smith, J.A., and Buehler, M., 2005b, "On the dynamics of bounding and extensions towards the half-bound and the gallop gaits," in *Adaptive Motion of Animals and Machines*, H. Kimura, K. Tsuchiya, A. Ishiguro, and H Witt, eds., Springer-Verlag, Tokyo, pp. 77–86.
- Raibert, M.H., 1985, "*Legged Robots that Balance*," MIT Press, Cambridge, MA.
- Saranli, U., Buehler, M., and Koditschek, D.E., 2001, "RHex: A simple and highly mobile hexapod robot," *International Journal of Robotics Research* **20**(7), 616–631.
- Serfarth, A., Geyer, H., Gunther, M., and Blickhan, R., 2002, "A movement criterion for running," *Journal Biomechan* **35**, 649–655.
- Taga, G., Yamaguchi, Y., and Shimizu, H., 1991, "Self-organized control of biped locomotion by neural oscillators," *Biological Cybernetics* **65**, 147–159.
- Vakakis, A.F., Burkick, J.W., and Caughey, T.K., 1991, "An interesting strange attractor in the dynamics of a hopping robot," *International Journal of Robotics Research* **10**(6), 606–618.
- Zhang, Z.G., Fukuoka, Y., and Kimura, H., 2003, "Adaptive running of a quadrupedal robot on irregular terrain based on biological concepts," in *Proceedings of the 2003 IEEE International Conference on Robotics and Automation*, pp. 2043–2048.
- Zhang, Z.G., Fukuoka, Y., and Kimura, H., 2005, "Adaptive running of a quadruped robot using delayed feedback control," in *Proceedings of the 2005 IEEE International Conference on Robotics and Automation*, pp. 3750–3755.